Original Article

Antibacterial Potential of Human Umbilical Cord Mesenchymal Stem Cell-Derived Exosomes Against *Clostridium Perfringens*: An Experimental *In Vitro* and *In Silico* Study

Sirous Banafi[1], DVM; Mohammad Hossein Marhamatizadeh[1], PhD; Nader Tanideh[2,3], PhD; Ebrahim Rahimi[1], PhD; Afshin Zare[4], MD; Ramazon Safarzoda Sharoffidin[5], PhD; Amin Tamadon[6,7,8], PhD

[1]Department of Food Hygiene, School of Veterinary Medicine, Kazerun Branch, Islamic Azad University, Kazerun, Iran;
[2]Stem Cells Technology Research Center, Shiraz University of Medical Sciences, Shiraz, Iran;
[3]Department of Pharmacology, School of Medicine, Shiraz University of Medical Sciences, Shiraz, Iran;
[4]International PhD Program in Medicine, College of Medicine, Taipei Medical University, Taipei, Taiwan;
[5]Department of Pharmaceutical Technology, Avicenna Tajik State Medical University, Dushanbe, Tajikistan;
[6]Department of Natural Sciences, West Kazakhstan Marat Ospanov Medical University, Aktobe, Kazakhstan;
[7]Stem Cells Technology Research Center, Shiraz University of Medical Sciences, Shiraz, Iran;
[8]PerciaVista R&D Co., Shiraz, Iran

Correspondence:
Mohammad Hossein Marhamatizadeh, PhD;
Department of Food Hygiene, School of Veterinary Medicine, Kazerun Branch, Islamic Azad University, Postal code: 74177-14131, Kazerun, Iran
Tel: +98 7212243930
Email: drmarhamati@gmail.com
Received: 13 March 2025
Revised: 22 August 2025
Accepted: 20 September 2025

What's Known

- In recent years, it has become evident that many of the beneficial effects of mesenchymal stem cells are mediated through their secreted exosomes—nanosized, phospholipid bilayer vesicles loaded with bioactive molecules, including nucleic acids, lipids, and proteins.

What's New

- *In silico* docking revealed strong binding affinities, particularly between the 70 kDa heat shock protein (Hsp70) and bacterial ribonucleic acid (RNA) polymerase (−1088.0 docking score) and adenosine triphosphate (ATP) synthase (−1021.4). Human umbilical cord mesenchymal stem cell–derived exosomes demonstrated potent anti-*C. perfringens* activity, likely mediated by interactions with essential bacterial enzymes.
- These findings highlighted their potential as a novel antimicrobial strategy.

Abstract

Background: *Clostridium perfringens* (*C. perfringens*) is an opportunistic anaerobic pathogen associated with severe soft tissue and gastrointestinal infections and increasing antimicrobial resistance. This study aimed to evaluate the *in vitro* antibacterial activity of human umbilical cord mesenchymal stem cell (hUC-MSC)-derived exosomes against *C. perfringens* and to explore potential exosome–enzyme interactions using *in silico* protein–protein docking.

Methods: This study was conducted at Shiraz University of Medical Sciences, Shiraz, Iran, in 2025. In this experimental *in vitro* and *in silico* study, human umbilical cord mesenchymal stem cells (hUC-MSCs) were isolated from term umbilical cords (UCs), characterized, and induced into osteogenic and adipogenic differentiation. Exosomes were isolated using a commercial precipitation kit and characterized by scanning electron microscopy (SEM), dynamic light scattering (DLS), and flow cytometry for CD63 expression. The antibacterial activity of exosomes against *C. perfringens* ATCC 2592 was evaluated by a broth microdilution minimum inhibitory concentration (MIC) assay under anaerobic conditions. Optical density (OD600) values were recorded and compared across exosome concentrations. Protein–protein docking was performed between exosomal proteins and four essential *C. perfringens* enzymes using ClusPro. OD600 values were compared across exosome concentrations using one-way analysis of variance (ANOVA) ($P<0.05$).

Results: hUC-MSCs displayed typical spindle-shaped morphology, tri-lineage differentiation potential, and a mesenchymal immunophenotype. Isolated exosomes were spherical nanovesicles (~30–100 nm) with high CD63 positivity. UC-MSC-derived exosomes inhibited *C. perfringens* growth in a dose-dependent manner. At 500 µg/mL, exosomes achieved 95.1% inhibition with an OD600 of 0.12±0.03 vs. 2.45±0.10 in the growth control ($n=3$, $P<0.001$). Docking analysis suggested favorable *in silico* interactions between Hsp70 and *C. perfringens* RNA polymerase and ATP synthase, and between cathelicidin and DNA gyrase, with lower but consistent docking scores for Annexin A1 across targets.

Conclusion: hUC-MSC-derived exosomes exerted significant *in vitro* antibacterial effects against *C. perfringens* and exhibited favorable *in silico* interactions with key bacterial enzymes.

Please cite this article as: Banafi S, Marhamatizadeh MH, Tanideh N, Rahimi E, Zare A, Safarzoda Sharoffidin R, Tamadon A. Antibacterial Potential of Human Umbilical Cord Mesenchymal Stem Cell-Derived Exosomes Against *Clostridium Perfringens*: An Experimental *In Vitro* and *In Silico* Study. Iran J Med Sci. doi: 10.30476/ijms.2026.108710.4369.

Keywords ● Exosomes ● Mesenchymal stem cells ● Umbilical cord ● *Clostridium perfringens* ● Anti-bacterial agents

Introduction

Clostridium perfringens is a common commensal of the human and animal gastrointestinal tract and contributes to shaping the gut microbial community.[1] However, under pathological conditions, it can translocate from mucosal surfaces—such as those of the nose, mouth, intestines, and urethra—to distant organs, including the lungs, bloodstream, brain, pancreas, and kidneys, potentially leading to severe infections, sepsis, and death.[1] Such dissemination is often associated with mucosal disruption caused by periodontal disease, respiratory impairment, or invasive medical procedures, including temporary or long-term implants.[2] Additionally, *C. perfringens* is an important pathogen in seafood-borne infections.[3]

Mesenchymal stem cells (MSCs) and their exosomes have recently gained attention for their antimicrobial potential. These vesicles can exert direct antibacterial effects through antimicrobial peptides and indirect effects through immunomodulation,[4] yet the activity of umbilical cord (UC)-MSC-derived exosomes specifically against *C. perfringens* has not been examined. Extracellular vesicles (EVs), including those released by microorganisms, play an important role in microbial competition and antibiotic resistance.[5, 6] Exosome-like vesicles from non-mammalian sources also exhibit antimicrobial activity; for example, honey-derived vesicles inhibit oral pathogens such as *Streptococcus mutans* and *Streptococcus sanguinis,*[7] while camel milk exosomes demonstrate antibacterial, antifungal, and anticancer effects and selectively increase oxidative stress in cancer cells.[8]

MSC-derived exosomes further contribute to inflammation regulation, infection control, and tissue repair.[9] Their low immunogenicity, stability, and efficient cargo delivery have made them promising platforms for drug and vaccine delivery.[10, 11] The biological activity of exosomes is strongly influenced by their cellular origin and physiological state.[12] Key antimicrobial factors within MSC exosomes include Annexin A1, cathelicidin, and heat shock protein 70 (Hsp70), which participate in immune modulation and direct microbial killing.[13] Conversely, *C. perfringens* relies on essential enzymes—including ATP synthase β, RNA polymerase β, DNA gyrase B, and MurA—for survival and virulence.[14, 15]

Given these considerations, the present study investigated the antibacterial activity of UC-MSC-derived exosomes against *C. perfringens* and explored potential molecular interactions between exosomal proteins and essential bacterial enzymes through *in silico* docking.

Materials and Methods

This study was approved by the Research Ethics Committee of Islamic Azad University, Kazerun Branch, under approval ID IR.IAU.KAU.REC.1404.059, dated 6 September 2025. This study was conducted in accordance with the Declaration of Helsinki. Written informed consent was obtained from all participants.

Isolation and Culture of UC-MSCs

Umbilical cords (UCs) were collected from five healthy mothers after full-term delivery at a defined hospital affiliated with the University of Medical Sciences. All samples were negative for hepatitis B, hepatitis C, human immunodeficiency virus (HIV), and syphilis. UCs were obtained from healthy term pregnancies (37–41 weeks of gestation) after elective cesarean section or vaginal delivery. Mothers with a history of chronic systemic disease, infectious disease during pregnancy, gestational diabetes, preeclampsia, or antibiotic use within the last weeks were excluded. UCs with visible signs of contamination or macroscopic abnormalities were not included. The UCs were stored in aseptic saline buffer, washed with phosphate-buffered saline (PBS) (ShellMaxx, Iran) containing 50 µg/mL streptomycin/penicillin, and maintained at 4°C until further use.

In the next step, veins, arteries, and any other adjacent tissues were removed from the cords, and the cords were chopped longitudinally into 2 mm pieces. Each piece was placed in a dish and allowed to adhere for approximately 30 min. The samples were then immersed in Dulbecco's Modified Eagle Medium/Nutrient Mixture F-12 (ShellMaxx, Iran) supplemented with 5% fetal bovine serum (FBS; Sigma-Aldrich, St. Louis, MO, USA), 2 mmol/L l-glutamine, and 50 U/mL penicillin/streptomycin, and incubated at 37°C in a 5% CO_2 humidified atmosphere. After 7 days, non-adherent cells were eliminated by washing, and the medium was changed twice a week thereafter. Subsequently, the FBS content of the medium was increased to 10%, and after 15 days, the UC fragments were removed from the dishes to allow cells to continue developing and proliferating. Once the cells reached 80–90% confluence, adherent cells were harvested using 0.05% trypsin/ ethylenediaminetetraacetic acid (EDTA; Gibco, Life Technologies, Carlsbad, CA, USA), and cultured until reaching the third passage. The culture of the UC-MSCs was morphologically monitored at defined time

points using an inverted microscope equipped with a digital camera.

Differentiation Potential of the UC-MSCs

The osteogenic and adipogenic differentiation potential of the UC-MSCs was assessed by exposing the cells to specific induction media. The osteogenic medium consisted of low-glucose DMEM, 15% FBS, 50 µg/mL ascorbic acid-2-phosphate (Merck, Germany), 100 nM dexamethasone (Sigma, USA), and 10 mM β-glycerophosphate (Merck, Germany). The adipogenic medium contained low-glucose DMEM, 15% FBS, 100 nM dexamethasone, 100 µM ascorbic acid, and 200 µM indomethacin (Sigma, USA). Both media were changed every 3 days. After 21 days, the cells were fixed with 4% formaldehyde for 15 minutes and stained with either Alizarin Red (40 mM, Sigma-Aldrich) or Oil Red O (0.5%, Sigma-Aldrich). The former stains calcium ions in mineralized deposits, resulting in a brilliant red color in newly formed osteocytes, while the latter stains the emerged adipocytes. Cells were visualized under light microscopy.

Expression of Surface Antigens by Flow Cytometry

The expression pattern of surface antigens on UC-MSCs was determined using a BD FACSCalibur™ flow cytometer (Becton, Dickinson and Company [BD], San Jose, CA, USA). Aliquots of 5×10^5 UC-MSCs at the third passage were labeled with a panel of monoclonal antibodies against cluster of differentiation CD73, CD90, CD34, and CD45. Briefly, cultured cells were harvested, washed by centrifugation in PBS, and resuspended in PBS buffer. The cells were then incubated with conjugated primary antibodies for 30 min at room temperature. After incubation, the expression of specific surface antigens was analyzed.

Exosome Isolation

UC-MSCs at the third passage were adapted to serum-free medium by gradually reducing the FBS content over 1 day. After 72 hours, the culture supernatant was collected and subjected to exosome isolation using a commercial kit (Exocib, Cibbiotech, Tehran, Iran) following the manufacturer's instructions. Briefly, the supernatant was first centrifuged at 300×g for 20 min and filtered through a 0.22 µm membrane. Reagent A was then added, and the mixture was incubated at 4 °C for approximately 12 hours. The sample was subsequently centrifuged at 3,000 rpm for 40 min. The resulting pellet was resuspended in 200 µL of Reagent B and stored at -70 °C.

Exosome Characterization by Scanning Electron Microscopy (SEM)

Approximately 25 µL of the exosome sample was initially fixed using a freeze dryer/lyophilizer (BIBASE, China). For SEM analysis, the exosomes were fixed with glutaraldehyde, dehydrated through a graded ethanol series, and air-dried at room temperature. The dried samples were then sputter-coated with a thin layer of gold to enhance conductivity and imaging quality. Finally, the morphology of the exosomes was examined using a scanning electron microscope (SEM; MIRA3 TESCAN, Brno, Czech Republic) after gold–palladium sputtering.

Quantification of the Protein Contents of the Exosomes

The bicinchoninic acid (BCA) assay is commonly used to quantify the protein concentration of samples by generating a standard curve. This method is based on the principle that proteins reduce Cu^{2}□ to Cu□ in an alkaline medium (the biuret reaction), leading to the formation of a purple-colored complex with bicinchoninic acid. The intensity of the color, which is proportional to the protein concentration, is measured by determining the optical density using a microplate reader. In this study, the protein content of the extracted exosome samples was quantified using a BCA Protein Quantification Kit (Parstous, Iran) following the manufacturer's instructions. Absorbance was measured using an Infinite M200 plate reader (Tecan Group Ltd., Männedorf, Switzerland).

Dynamic light Scattering (DLS)

Dynamic light scattering (DLS) is an efficient, non-invasive technique used to assess the size distribution and homogeneity of exosomes. Unlike other methods, DLS does not require pre-treatment steps, such as staining or fixation, making it a convenient approach for analyzing exosomal preparations. In this method, the isolated exosomes were diluted to a concentration of 0.1 µg/µL and transferred into a cuvette, which was then filled to a final volume of 100 µL using PBS. The sample was analyzed using a DLS instrument (Nano Zetasizer, Model SZ-100, HORIBA, Japan) to determine the particle size distribution.

Exosome Characterization Through Expression of Specific Surface Antigens by Flow cytometry

Exosomes possess characteristic multi-transmembrane surface proteins.[16] To confirm their presence following isolation, the expression of the tetraspanin CD63 was evaluated using flow cytometry.

Antimicrobial Activity of UC-MSCs-Derived Exosomes on C. Perfringens

The antimicrobial activity of exosomes derived from human UC-MSCs against *C. perfringens* (ATCC 2592) was assessed by determining the minimum inhibitory concentration (MIC) using a modified broth microdilution method, based on Clinical and Laboratory Standards Institute (CLSI) guidelines.[17] The MIC assay was performed in Mueller–Hinton broth/Roswell Park Memorial Institute (RPMI) supplemented with additives, according to CLSI recommendations adapted for anaerobic bacteria.

An overnight culture of *C. perfringens* in brain–heart infusion supplemented (BHIS) broth was diluted 1:50 in fresh BHIS and incubated until the optical density at 600 nm (OD600 ≈0.35). The working bacterial suspension was prepared by diluting the stock culture 1:1000 in Mueller–Hinton broth. All MIC plates were incubated at 37°C for 24 h in an anaerobic jar system (GasPak EZ Anaerobe Container System, BD Diagnostics, USA) under an atmosphere of 80% N_2, 10% H_2, 10% CO_2.

Final exosome concentrations in MIC wells were 125, 250, 450, and 500 µg/mL. Each well of the microtiter plate contained 0.1 mL of the standardized bacterial suspension adjusted to 1–5×10^5 CFU/mL. Growth control wells contained the same bacterial suspension without exosomes, and blank control wells contained medium alone. Exosomes were serially diluted in Mueller-Hinton broth to achieve the final concentrations. Bacterial suspensions (1–5×10^6 cells/mL and 1–1.5×10^8 cells/mL) were prepared by suspending three colonies of *C. perfringens* in 5 mL of sterile 0.85% NaCl. The turbidity of the inoculum was adjusted to match a 0.5 McFarland standard at a wavelength of 630 nm.

An overnight culture was diluted 1:50 in fresh brain–heart infusion-supplemented (BHIS) broth and incubated until the optical density at 600 nm (OD600) reached approximately 0.35. The working suspension was then prepared by diluting the stock culture 1:1,000 in RPMI or 1:100 in Mueller-Hinton broth.

Each well of a microtiter plate was inoculated with 0.1 mL of the working suspension and incubated at 37°C for 0 and 24 hours in an anaerobic jar. Blank controls (media only) and growth controls (media with inoculum but without exosomes) were included for comparison. Microbial growth was visually assessed in each well against the corresponding growth control. The MIC was defined as the lowest concentration of exosomes resulting in ≥95% inhibition of visible bacterial growth compared to the growth control. All experiments were performed in triplicate.

Each plate included blank control wells (medium without bacteria or exosomes), growth control wells (medium with bacterial inoculum but without exosomes), and vehicle control wells where applicable. Exosome-treated wells contained the same final volume and medium composition as the controls.

Protein Sequence Retrieval and Molecular Modeling

The FAST-All Sequence Format (FASTA) sequences of the target proteins—antibacterial proteins derived from human umbilical cord mesenchymal stem cells (hUC-MSCs) and survival-associated proteins of *C. perfringens*—were retrieved from the UniProt database (https://www.uniprot.org/). Molecular models of each protein were generated via homology modeling using the SWISS-MODEL online tool (https://swissmodel.expasy.org/). The resulting structures were subsequently subjected to energy minimization and chain optimization using ViewerLite software (Accelrys Inc., San Diego, CA, USA) to enhance structural integrity.

Protein-Protein Docking Analysis

Protein–protein docking was conducted between antibacterial proteins derived from hUC-MSCs and essential survival proteins of *C. perfringens* using the ClusPro Protein–Protein Docking Server (ClusPro) online server (https://cluspro.bu.edu/). ClusPro utilizes a rigid-body docking algorithm, followed by clustering of the lowest-energy conformations to predict the most probable protein–protein interactions. Docking scores for the top-ranked complexes were recorded and are presented in table 1.

Visualization and Interaction Analysis

The docked complexes were analyzed using the Protein Data Bank Summary Database (PDBsum) (http://www.ebi.ac.uk/pdbsum/) to identify key amino acid residues involved in molecular interactions, including hydrogen bonds, hydrophobic contacts, and salt bridges. For clarity and visualization, structural representations of the docked complexes were generated using Python Molecular Graphics System (PyMOL, version 2.0, Schrödinger, LLC., New York, NY, USA) and the PDBsum online tool.

Statistical and Bioinformatic Validation

The docking results were evaluated based on binding energy scores and cluster population density, as provided by ClusPro. The most stable complexes were identified by selecting those with the lowest-energy conformations and the highest cluster occupancies.

Table 1: Docking scores of the top-ranked complexes obtained from ClusPro

Name of protein	Organism	UniProt ID	Coding gene	Reference
Annexin A1	hUC-MSC Exosomes	P04083 · ANXA1_HUMAN	ANXA1	18
Cathelicidin antimicrobial peptide	hUC-MSC Exosomes	P49913 · CAMP_HUMAN	CAMP	19
Hsp70	hUC-MSC Exosomes	P0DMV8 · HS71A_HUMAN	HSPA1A	20
ATP synthase subunit beta	*C. perfringens*	Q0TNC4 · ATPB_CLOP1	atpD	21
DNA-directed RNA polymerase subunit beta	C. perfringens	P0C2E7 · RPOB_CLOPE	rpoB	22
DNA gyrase subunit B	*C. perfringens*	Q8XPF7 · Q8XPF7_CLOPE	gyrB	23
UDP-N-acetylglucosamine 1-carboxyvinyltransferase 2	*C. perfringens*	A0A0H2YMZ3 · A0A0H2YMZ3_CLOP1	murA	24

ANXA1: Annexin A1 gene; CAMP: Cathelicidin antimicrobial peptide gene; HSPA1A: Heat shock protein family A member 1A gene

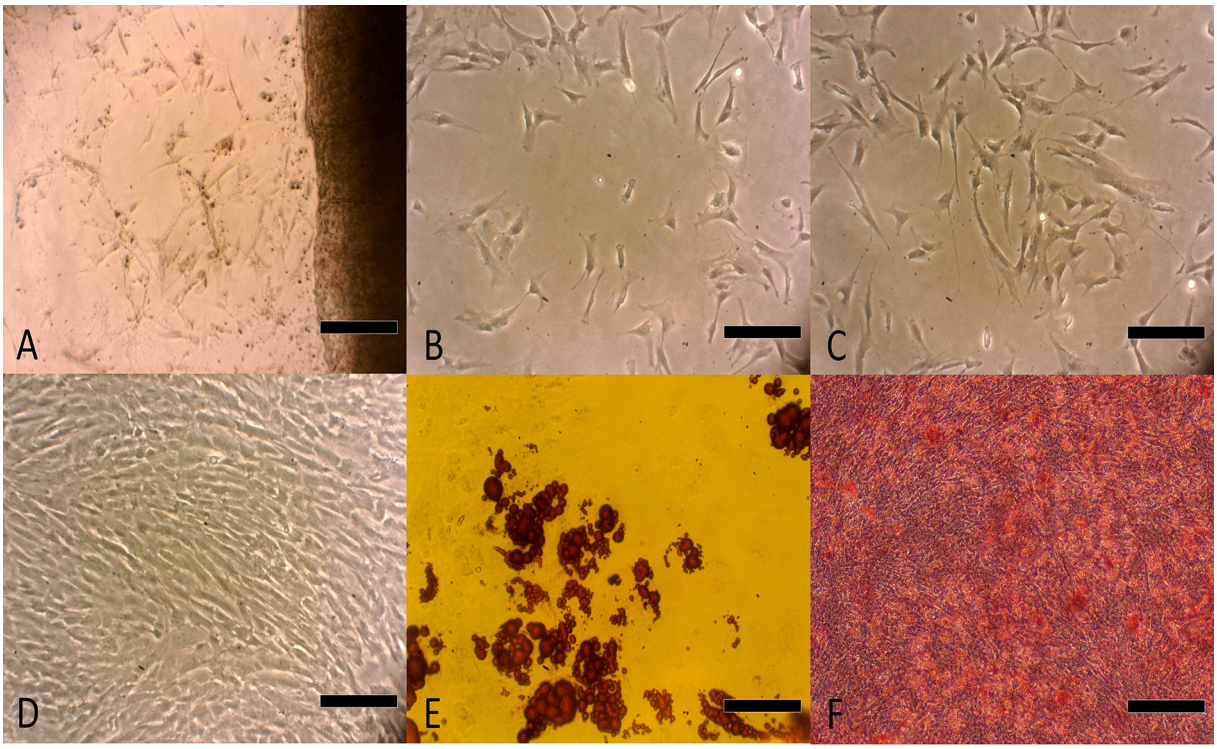

Figure 1: This figure illustrates the morphological characteristics and differentiation potential of human umbilical cord mesenchymal stem cells (hUC-MSCs). A: Adherent cells are observed emerging from the edges of umbilical cord explants between days 3 and 12 of culture. B: Migrating cells form a confluent monolayer culture around the explants. C: Cells reach approximately 80% confluence after 12-21 days and exhibit a spindle-shaped, fibroblast-like morphology typical of MSCs. D: Control cells at passage 3 (P3) retain fibroblastic morphology when maintained in basal medium. E: Cells cultured in osteogenic induction medium and stained with Alizarin Red after 21 days show calcium deposition consistent with osteogenic differentiation. F: Cells cultured in adipogenic induction medium and stained with Oil Red O display intracellular lipid droplets indicative of adipogenic differentiation. Scale bars=200µm

All data were tabulated and analyzed using GraphPad Prism 9 (GraphPad Software, San Diego, CA, USA). After identifying outliers and assessing data normality, statistical significance was determined using one-way analysis of variance (ANOVA), with a significance threshold set at $P<0.05$. For the MIC assay, OD600 values from triplicate wells were summarized as mean±SD and compared across groups (control and exosome concentrations) using one-way ANOVA.

Results

hUC-MSCs Culture and Characterization

hUC-MSCs migrated from umbilical cord explants and established adherent monolayer cultures. They displayed a spindle-shaped morphology and successfully differentiated into osteogenic and adipogenic lineages, confirming their multipotency (figure 1).

Flow cytometry analysis confirmed that the isolated and expanded cells were positive for MSC markers (CD73, and CD90) and negative for hematopoietic markers (CD34, and CD45; figure 2).

SEM Analysis of the UC-MSCs Exosomes

SEM imaging confirmed a typical exosomal morphology, revealing spherical nanovesicles within the expected size range (figure 3).

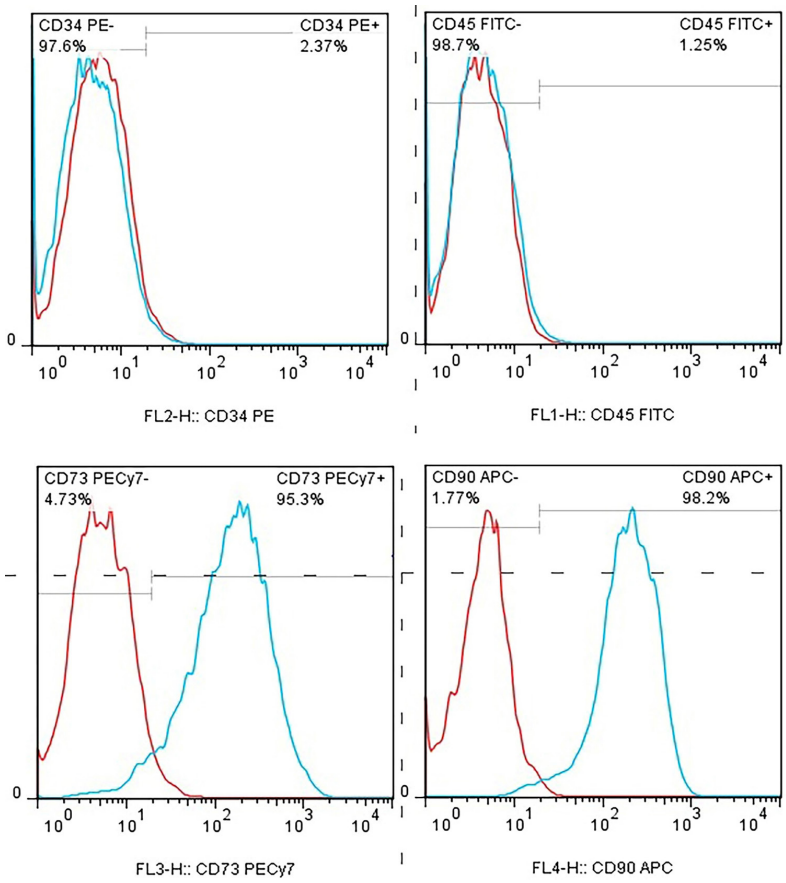

Figure 2: This figure illustrates the flow cytometric analysis of surface marker expression in human umbilical cord mesenchymal stem cells (hUC-MSCs). The cells show high expression of MSC markers CD73 and CD90, confirming their mesenchymal phenotype. They are negative for the hematopoietic markers CD34 and CD45, indicating the absence of hematopoietic contamination in the cultured population.

Bicinchoninic Acid (BCA) Assay

The BCA assay demonstrated a protein concentration of 1.123 µg/mL for the exosome preparation (figure 4).

Dynamic Light Scattering (DLS) Results

DLS analysis indicated a predominantly uniform size distribution for the exosomes, consistent with that of nanoscale vesicles (figure 5).

Exosome Characterization

Flow cytometry analysis confirmed the presence of the exosome-specific marker CD63 in the isolated sample (figure 6). The results demonstrated that 81.5% of the particles were positive for CD63, indicating high exosome purity. Additionally, 80.5% of events fell within the main population gate (Forward Scatter Hight [FSC-H] vs. FSC-H), suggesting consistent particle size distribution. CD63 was the only exosomal surface marker evaluated in this study. These findings validated the successful isolation and characterization of exosomes based on surface marker expression.

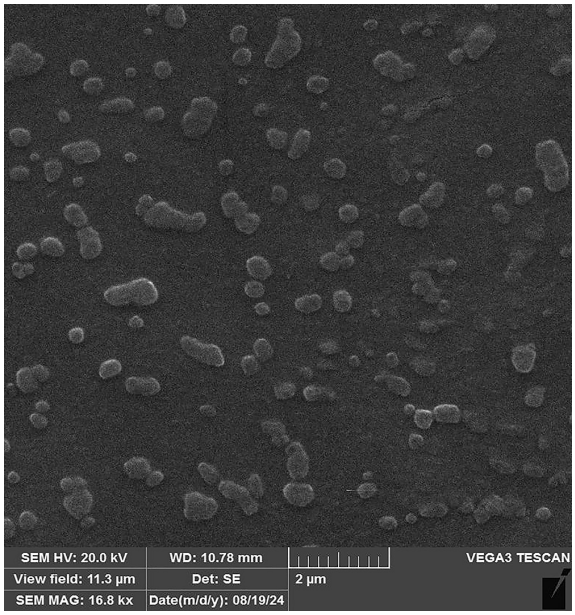

Figure 3: This figure illustrates the scanning electron microscopy (SEM) images of exosomes derived from human umbilical cord mesenchymal stem cells (hUC-MSCs). The purified vesicles appear as round, spheroid nanovesicles lacking a central depression, with diameters ranging from approximately 30 to 100 nm, consistent with typical exosome morphology.

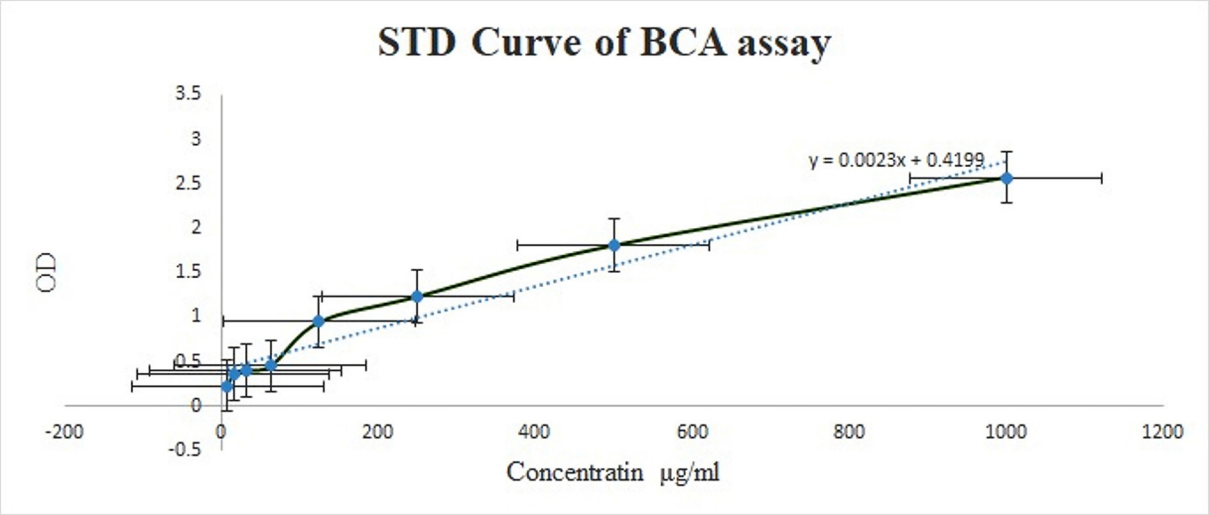

Figure 4: This figure illustrates the standard curve of the bicinchoninic acid (BCA) assay for protein quantification of exosomes derived from human umbilical cord mesenchymal stem cells (hUC-MSCs). The linear regression equation (y=0.0023x+0.4199) was used to calculate the total protein concentration of the exosome preparation. Data points represent mean absorbance values±standard deviation (SD) from three independent measurements (n=3).

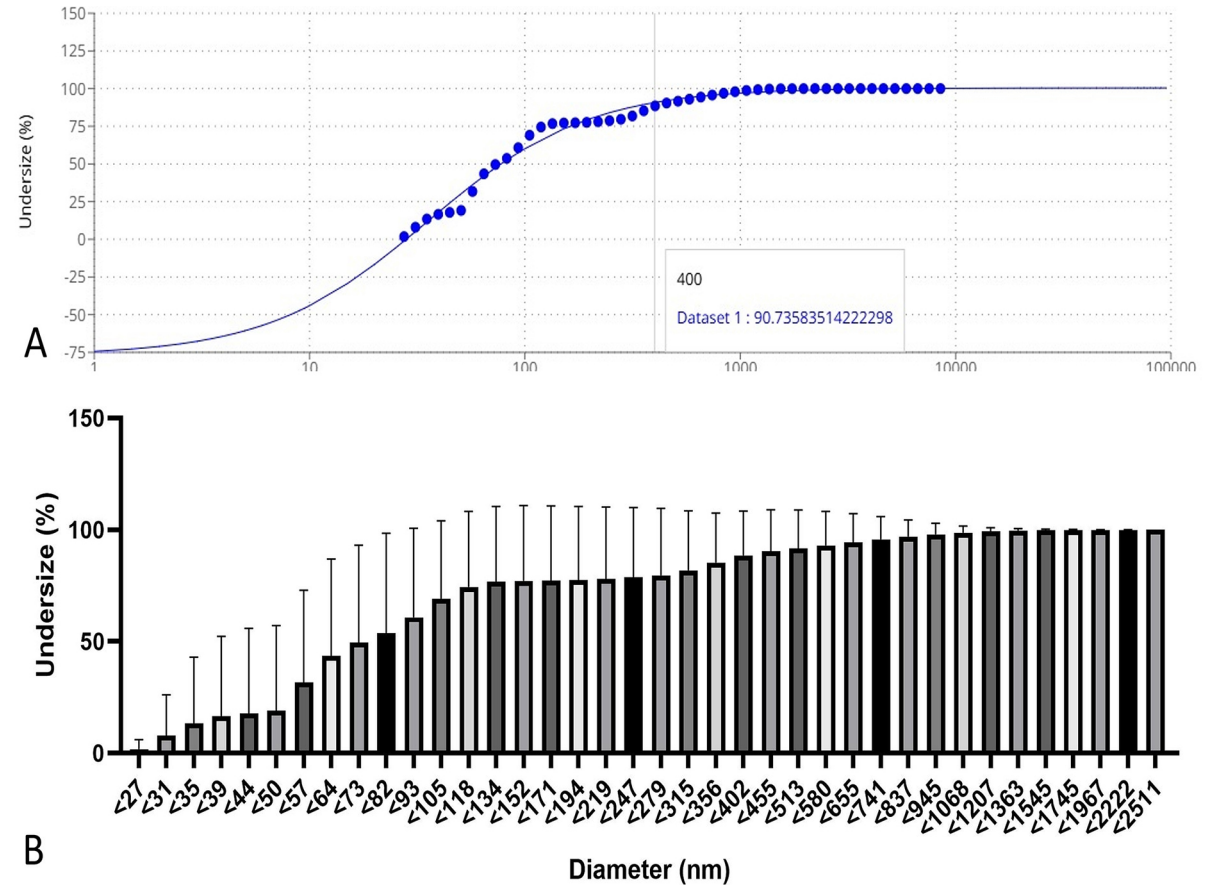

Figure 5: This figure illustrates the particle size distribution of exosomes derived from human umbilical cord mesenchymal stem cells (hUC-MSCs) analyzed by dynamic light scattering (DLS). A: The undersize percentage curve shows the cumulative distribution of particle diameters in the exosome preparation. B: A representative intensity-based size distribution plot demonstrates a predominant peak near 100 nm. The combined data confirm that approximately 90% of particles have diameters below 400 nm, consistent with the expected size range of exosomes.

Antimicrobial Properties of the UC-MSCs-Derived Exosomes

Investigating the antibacterial activity of exosomes on *C. perfringens* revealed significant, concentration-dependent inhibition of bacterial growth. At 500 µg/mL, exosomes achieved 95.1% inhibition (OD600: 0.12±0.03) compared to the growth control (2.45±0.10, n=3).

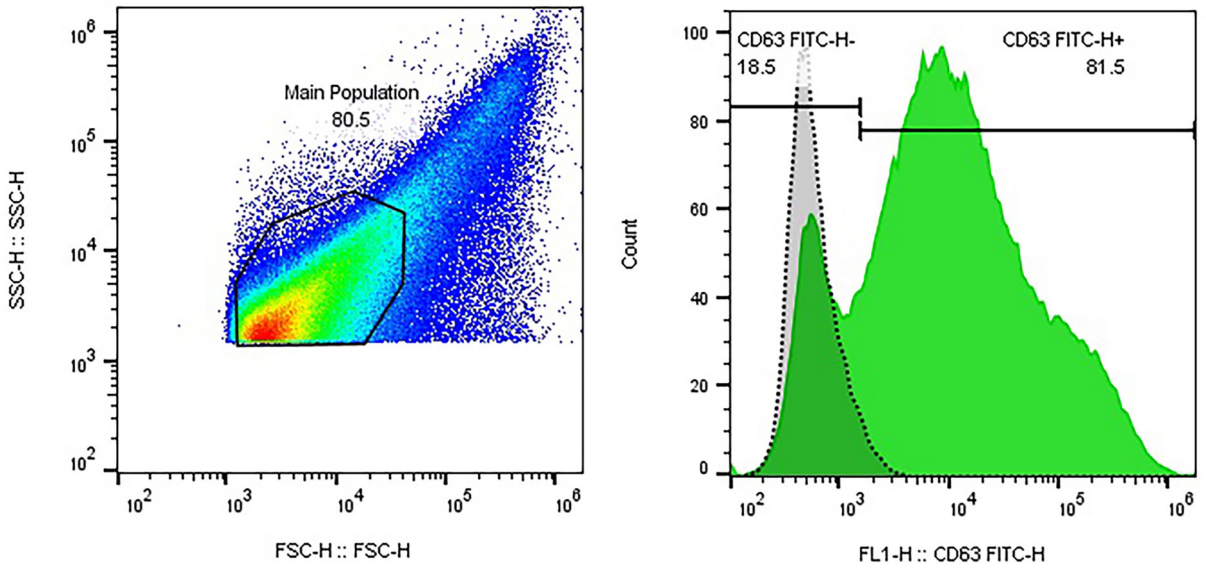

Figure 6: This figure illustrates the flow cytometric characterization of exosome surface marker CD63. Forward scatter height (FSC-H) versus forward scatter area (FSC-A) gating identifies the main exosome population, comprising 80.5% of recorded events. Histogram analysis of CD63-FITC fluorescence (FL1-H) shows that 81.5% of gated particles are positive for CD63, confirming the exosomal nature of the isolated vesicles.

Table 2: Docking scores of human umbilical cord mesenchymal stem cells (hUC-MSCs)-derived proteins against *C. perfringens* survival proteins

Essential bacterial enzymes	**Exosomal antimicrobial proteins**		
	Annexin A1	Cathelicidin **antimicrobial peptide**	Hsp70
ATP synthase subunit beta	-635.6	-764.3	-1021.4
DNA-directed RNA polymerase subunit beta	-787.6	-845.9	-1088.0
DNA gyrase subunit B	-760.6	-795.0	-969.6
UDP-N-acetylglucosamine 1-carboxyvinyltransferase 2	-708.8	-610.5	-900.5

Hsp70: Heat shock protein 70; ATP: Adenosine triphosphate; RNA: Ribonucleic acid; UDP: Uridine diphosphate

One-way ANOVA demonstrated a significant difference in OD600 among the tested concentrations and controls ($P<0.001$). Inhibition decreased at lower concentrations (e.g., MIC 0.5=44.0% and MIC 0.25=35.6%).

Computational Protein-Protein Docking

Protein-protein docking was performed between three hUC-MSC proteins with known antibacterial effects (Annexin A1, Cathelicidin antimicrobial peptide, and Hsp70) and four essential *C. perfringens* survival proteins (ATP synthase subunit beta (atpD), DNA-directed RNA polymerase subunit beta (rpoB), DNA gyrase subunit B (gyrB), and UDP-N-acetylglucosamine 1-carboxyvinyltransferase 2 (murA). The docking scores (in arbitrary energy units) obtained from ClusPro are summarized in table 2.

The results indicated potentially favorable interactions between the hUC-MSC-derived proteins and *C. perfringens* targets, with Hsp70 exhibiting the highest binding affinity across all bacterial proteins, particularly against DNA-directed RNA polymerase subunit beta (-1088.0) and ATP synthase subunit beta (-1021.4). Cathelicidin also showed significant interactions, especially with DNA-directed RNA polymerase subunit beta (-845.9) and DNA gyrase subunit B (-795.0), while Annexin A1 displayed moderate but consistent binding. Moreover, detailed data on interacting amino acid residues between hUC-MSC-derived proteins and *C. perfringens* proteins are depicted in figure 7.

Discussion

This study provided the first evidence that exosomes derived from hUC-MSCs possess direct antibacterial activity against *C. perfringens*. The vesicles exhibited typical exosomal morphology, size distribution, and CD63 expression, and they inhibited *C. perfringens* growth in a dose-dependent manner, achieving nearly complete suppression at the highest concentration tested. This dose–response relationship aligned with recent studies demonstrating that the antimicrobial efficacy of MSC-derived secretomes and extracellular vesicles increased with vesicle concentration and protein cargo density.[25]

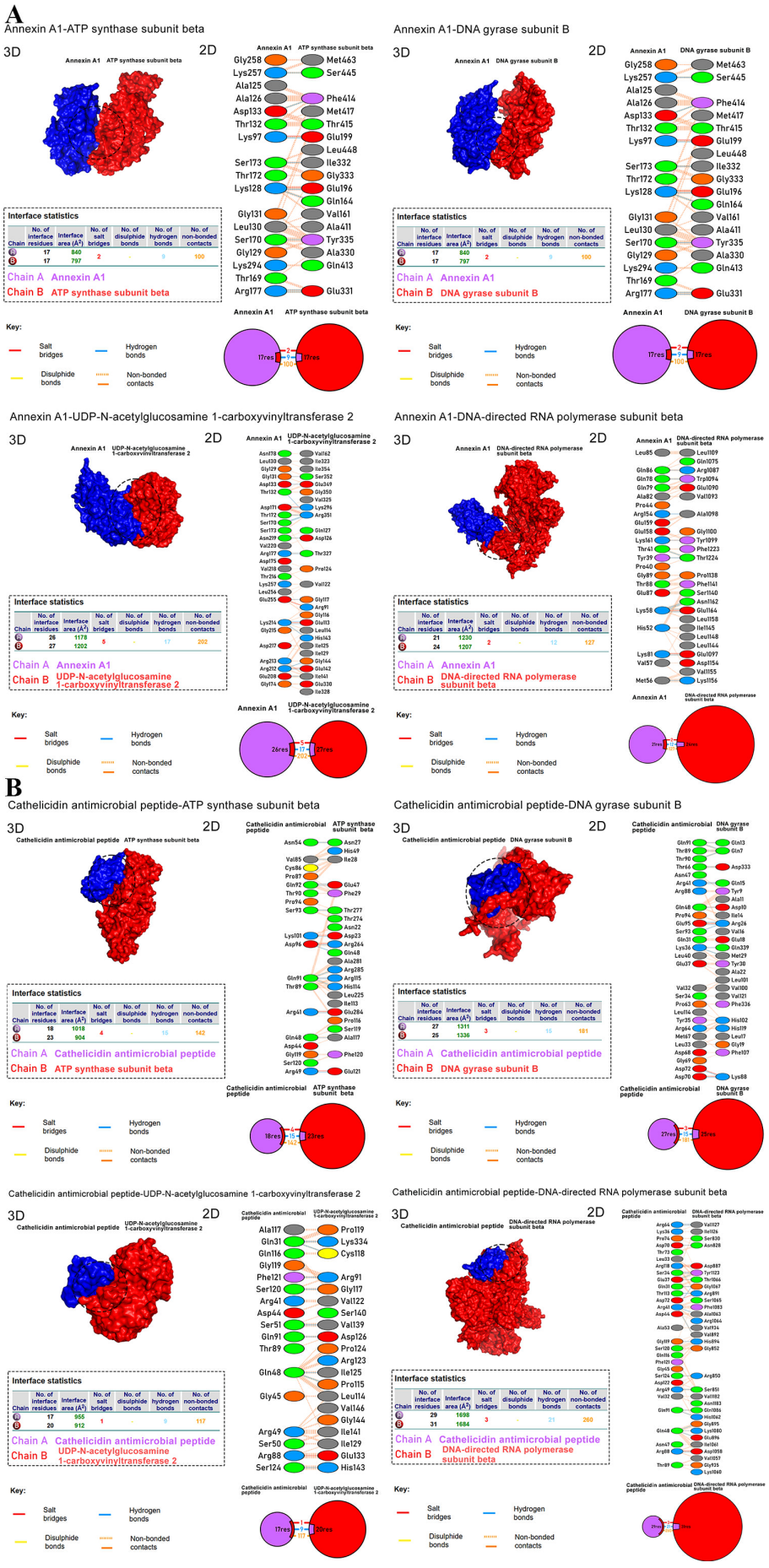
A
Annexin A1-ATP synthase subunit beta
3D
2D
Annexin A1 ATP synthase subunit beta
Interface statistics
Chain A Annexin A1
Chain B ATP synthase subunit beta
Key:
Salt bridges
Hydrogen bonds
Disulphide bonds
Non-bonded contacts
Annexin A1-DNA gyrase subunit B
Annexin A1 DNA gyrase subunit B
Chain A Annexin A1
Chain B DNA gyrase subunit B
Annexin A1-UDP-N-acetylglucosamine 1-carboxyvinyltransferase 2
Annexin A1 UDP-N-acetylglucosamine 1-carboxyvinyltransferase 2
Chain A Annexin A1
Chain B UDP-N-acetylglucosamine 1-carboxyvinyltransferase 2
Annexin A1-DNA-directed RNA polymerase subunit beta
Annexin A1 DNA-directed RNA polymerase subunit beta
Chain A Annexin A1
Chain B DNA-directed RNA polymerase subunit beta
B
Cathelicidin antimicrobial peptide-ATP synthase subunit beta
Cathelicidin antimicrobial peptide ATP synthase subunit beta
Chain A Cathelicidin antimicrobial peptide
Chain B ATP synthase subunit beta
Cathelicidin antimicrobial peptide-DNA gyrase subunit B
Cathelicidin antimicrobial peptide DNA gyrase subunit B
Chain A Cathelicidin antimicrobial peptide
Chain B DNA gyrase subunit B
Cathelicidin antimicrobial peptide-UDP-N-acetylglucosamine 1-carboxyvinyltransferase 2
Cathelicidin antimicrobial peptide UDP-N-acetylglucosamine 1-carboxyvinyltransferase 2
Chain A Cathelicidin antimicrobial peptide
Chain B UDP-N-acetylglucosamine 1-carboxyvinyltransferase 2
Cathelicidin antimicrobial peptide-DNA-directed RNA polymerase subunit beta
Cathelicidin antimicrobial peptide DNA-directed RNA polymerase subunit beta
Chain A Cathelicidin antimicrobial peptide
Chain B DNA-directed RNA polymerase subunit beta

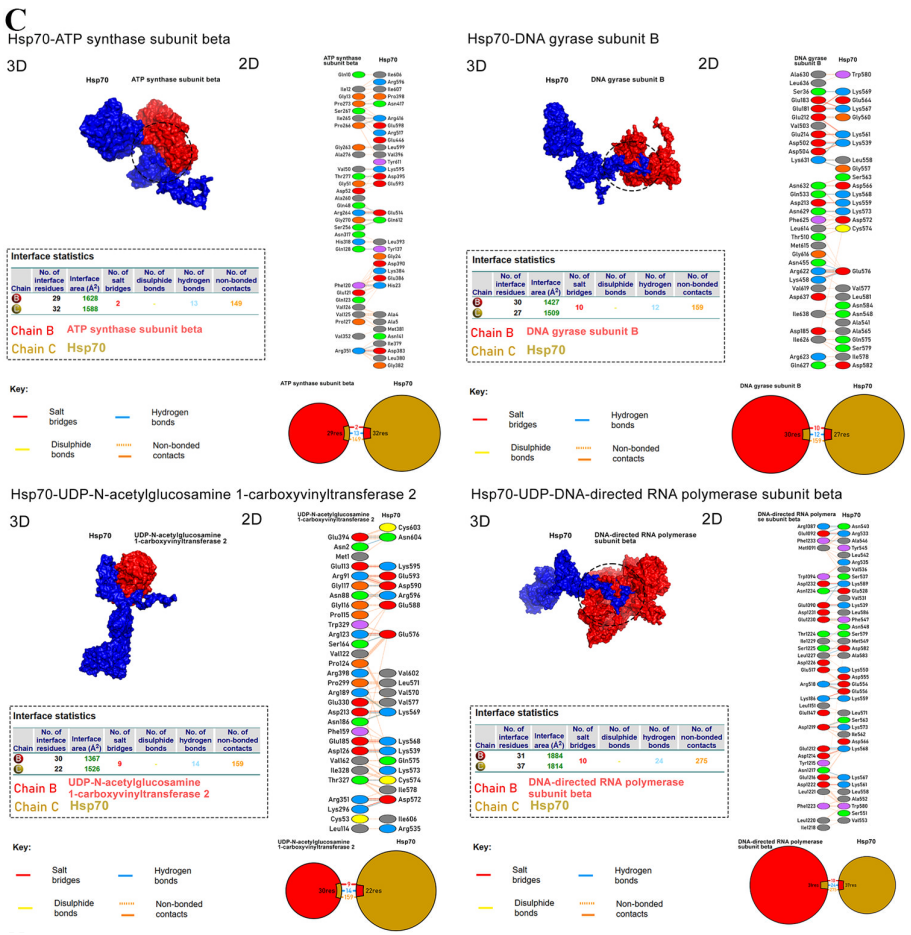

Figure 7: This figure illustrates the representative protein–protein docking models of exosomal proteins with *Clostridium perfringens* enzymes. A: Annexin A1 docked to ATP synthase subunit β. Models were visualized using PyMOL, and interacting residues were identified with PDBsum. B: Cathelicidin antimicrobial peptide docked to DNA gyrase subunit B, with principal contacts indicated. C: Hsp70 (surface in blue) docked to RNA polymerase β subunit (surface in grey), highlighting key interface residues (sticks) involved in hydrogen bonding and hydrophobic interactions.

Comparatively, previous investigations reported antibacterial activity of MSC-derived exosomes primarily against aerobic or facultative pathogens such as *Staphylococcus aureus*, *Escherichia coli*, and *Pseudomonas aeruginosa*, with limited data on obligate anaerobes.[13] In this context, our findings extended the antimicrobial spectrum of MSC-derived exosomes to *C. perfringens*, a clinically relevant anaerobic pathogen associated with foodborne illness, gas gangrene, and sepsis. Unlike many earlier studies in which exosomes were engineered or loaded with antibiotics to achieve antimicrobial efficacy, our data demonstrated intrinsic antibacterial activity of naïve UC-MSC exosomes, highlighting a key distinction from drug-loaded exosome strategies reported for Mycobacterium tuberculosis and methicillin-resistant *S. aureus*.[26] Given the rising burden of antimicrobial resistance and the limited treatment options for anaerobic pathogens, UC-MSC exosomes may represent a promising cell-free antimicrobial approach.[4, 25]

Previous studies showed variable antimicrobial effects of exosomes depending on their source and the targeted microorganism.[4, 16] Some exosomes demonstrated intrinsic activity, while others required therapeutic loading—for example, rifampicin- or linezolid-loaded exosomes improved clearance of *Mycobacterium tuberculosis* and MRSA, respectively.[26, 27] The present study expanded on these findings by demonstrating intrinsic antibacterial activity of UC-MSC exosomes with no drug loading, suggesting that endogenous proteins may contribute to this effect.

Mechanistically, the intrinsic antibacterial effect observed in this study might be partially explained by the protein cargo of UC-MSC-derived exosomes. Previous studies identified antimicrobial peptides and immune-modulatory proteins—including cathelicidin (LL-37), Annexin A1, and heat shock protein 70 (Hsp70)—as functional components of MSC secretomes that can contribute to antibacterial activity.[19] In line with these reports, the present *in silico*

docking analysis predicted stable interactions between these exosomal proteins and essential *C. perfringens* enzymes involved in transcription (RNA polymerase), energy metabolism (ATP synthase), and DNA replication (DNA gyrase). However, it should be emphasized that protein–protein docking provides preliminary, hypothesis-generating insights; rigid docking does not fully account for protein dynamics, cellular context, or environmental conditions, and therefore these predicted interactions require biochemical and functional validation.[16]

Importantly, differences between our findings and previous reports should also be considered. Some studies suggested that MSC-derived exosomes exert antibacterial effects predominantly through indirect immunomodulatory mechanisms rather than direct bacterial growth inhibition.[4, 9] In contrast, the present study demonstrated direct growth suppression in a cell-free *in vitro* system, indicating that UC-MSC exosomes could act independently of host immune cells. This discrepancy might reflect differences in MSC source, isolation methods, vesicle cargo composition, or pathogen type, all of which are known to influence exosome bioactivity.[16]

Despite encouraging results, several challenges must be addressed before translation. Standardization of exosome isolation and characterization remains critical due to the heterogeneity of MSC-derived products.[16] Our characterization strategy confirmed vesicle morphology, size range, and CD63 expression. However, it did not include additional positive or negative markers recommended by MISEV2023, nor did we profile the protein or RNA cargo. Consequently, attribution of antibacterial activity to specific exosomal proteins remains speculative. Cytotoxicity toward mammalian cells was not assessed, and no antibiotic comparator was included in the MIC assay, limiting interpretation of relative potency. Furthermore, the *in vitro* model could not replicate immune responses or physiological conditions encountered during infection. Overall, these findings provided a rationale for advancing UC-MSC exosomes into *in vivo* models of *C. perfringens* infection and evaluating synergistic effects with conventional antimicrobials.

Conclusion

The hUC-MSC-derived exosomes demonstrated potent, concentration-dependent antibacterial activity against *C. perfringens*, achieving up to 95% inhibition *in vitro*. Computational docking suggested potential *in silico* interactions between exosomal proteins—particularly Hsp70 and cathelicidin—and essential bacterial enzymes involved in transcription, energy metabolism, and DNA replication. Nonetheless, these predictions require experimental confirmation. Although preliminary, these results highlighted UC-MSC exosomes as a promising cell-free antimicrobial platform. Future studies should include cytotoxicity testing, antibiotic comparators, and *in vivo* validation, as well as optimization of exosome engineering and delivery strategies to enhance therapeutic potential.

Acknowledgment

The authors gratefully acknowledge the facilities and support provided by their affiliated institutions. This study was conducted as part of the PhD thesis of Sirous Banafi, at the Faculty of Veterinary Medicine, Kazerun Branch, Islamic Azad University, Kazerun, Iran. The PhD project and the present study were self-funded by the first author, and no external grant or institutional funding was received.

Authors' Contribution

S.B: Conceptualization, methodology, investigation, writing–original draft preparation; H.M: Conceptualization, writing–review and Editing, supervision, N.T: methodology, writing–review and editing, supervision; E.R: Investigation, writing–review and editing; A.Z: Methodology, formal analysis, *in silico* analysis, writing – review and editing; R.S.S: Investigation, data curation, writing–review and editing; A.T: Conceptualization, writing–review and editing, supervision, project administration. All authors have read and approved the final manuscript and agree to be accountable for all aspects of the work in ensuring that questions related to the accuracy or integrity of any part of the work are appropriately investigated and resolved.

Declaration of AI

The authors declare that artificial intelligence (AI)-assisted technologies, specifically a large language model (ChatGPT, OpenAI), were used to assist in language editing, formatting, and structuring of the manuscript text. All scientific content, study design, data collection, analyses, and conclusions were developed and verified by the authors.

Conflict of Interest: None declared.

References

1 Ba X, Jin Y, Ning X, Gao Y, Li W, Li Y, et al. Clostridium perfringens in the Intestine:

Innocent Bystander or Serious Threat? Microorganisms. 2024;12. doi: 10.3390/microorganisms12081610. PubMed PMID: 39203452; PubMed Central PMCID: PMC11356505.
2 Yadav S, Parihar A, Sadique MA, Ranjan P, Kumar N, Singhal A, et al. Emerging point-of-care optical biosensing technologies for diagnostics of microbial infections. ACS Appl Opt Mater. 2023;1:1245-62. doi: 10.1021/acsaom.3c00129.
3 Grenda T, Jarosz A, Sapała M, Grenda A, Patyra E, Kwiatek K. Clostridium perfringens-Opportunistic Foodborne Pathogen, Its Diversity and Epidemiological Significance. Pathogens. 2023;12. doi: 10.3390/pathogens12060768. PubMed PMID: 37375458; PubMed Central PMCID: PMC10304509.
4 Hoseinzadeh A, Esmaeili SA, Sahebi R, Melak AM, Mahmoudi M, Hasannia M, et al. Fate and long-lasting therapeutic effects of mesenchymal stromal/stem-like cells: mechanistic insights. Stem Cell Res Ther. 2025;16:33. doi: 10.1186/s13287-025-04158-z. PubMed PMID: 39901306; PubMed Central PMCID: PMC11792531.
5 Jiang B, Lai Y, Xiao W, Zhong T, Liu F, Gong J, et al. Microbial extracellular vesicles contribute to antimicrobial resistance. PLoS Pathog. 2024;20:e1012143. doi: 10.1371/journal.ppat.1012143. PubMed PMID: 38696356; PubMed Central PMCID: PMC11065233.
6 Pérez J, Contreras-Moreno FJ, Marcos-Torres FJ, Moraleda-Muñoz A, Muñoz-Dorado J. The antibiotic crisis: How bacterial predators can help. Comput Struct Biotechnol J. 2020;18:2547-55. doi: 10.1016/j.csbj.2020.09.010. PubMed PMID: 33033577; PubMed Central PMCID: PMC7522538.
7 Leiva-Sabadini C, Alvarez S, Barrera NP, Schuh C, Aguayo S. Antibacterial Effect of Honey-Derived Exosomes Containing Antimicrobial Peptides Against Oral Streptococci. Int J Nanomedicine. 2021;16:4891-900. doi: 10.2147/ijn.s315040. PubMed PMID: 34321877; PubMed Central PMCID: PMC8312616.
8 Shaban AM, Raslan M, Sharawi ZW, Abdelhameed MS, Hammouda O, El-Masry HM, et al. Antibacterial, Antifungal, and Anticancer Effects of Camel Milk Exosomes: An In Vitro Study. Vet Sci. 2023;10. doi: 10.3390/vetsci10020124. PubMed PMID: 36851428; PubMed Central PMCID: PMC9963947.
9 Zhankina R, Baghban N, Askarov M, Saipiyeva D, Ibragimov A, Kadirova B, et al. Mesenchymal stromal/stem cells and their exosomes for restoration of spermatogenesis in non-obstructive azoospermia: a systemic review. Stem Cell Res Ther. 2021;12:229. doi: 10.1186/s13287-021-02295-9. PubMed PMID: 33823925; PubMed Central PMCID: PMC8025392.
10 Fathi-Karkan S, Heidarzadeh M, Narmi MT, Mardi N, Amini H, Saghati S, et al. Exosome-loaded microneedle patches: Promising factor delivery route. Int J Biol Macromol. 2023;243:125232. doi: 10.1016/j.ijbiomac.2023.125232. PubMed PMID: 37302628.
11 Lener T, Gimona M, Aigner L, Börger V, Buzas E, Camussi G, et al. Applying extracellular vesicles based therapeutics in clinical trials - an ISEV position paper. J Extracell Vesicles. 2015;4:30087. doi: 10.3402/jev.v4.30087. PubMed PMID: 26725829; PubMed Central PMCID: PMC4698466.
12 Tomokiyo A, Wada N, Maeda H. Periodontal Ligament Stem Cells: Regenerative Potency in Periodontium. Stem Cells Dev. 2019;28:974-85. doi: 10.1089/scd.2019.0031. PubMed PMID: 31215350.
13 Izadi M, Dehghan Marvast L, Rezvani ME, Zohrabi M, Aliabadi A, Mousavi SA, et al. Mesenchymal Stem-Cell Derived Exosome Therapy as a Potential Future Approach for Treatment of Male Infertility Caused by Chlamydia Infection. Front Microbiol. 2021;12:785622. doi: 10.3389/fmicb.2021.785622. PubMed PMID: 35095800; PubMed Central PMCID: PMC8792933.
14 Elnar AG, Kim GB. Complete genome sequence of Clostridium perfringens B20, a bacteriocin-producing pathogen. J Anim Sci Technol. 2021;63:1468-72. doi: 10.5187/jast.2021.e113. PubMed PMID: 34957460; PubMed Central PMCID: PMC8672250.
15 AlJindan R, AlEraky DM, Farhat M, Almandil NB, AbdulAzeez S, Borgio JF. Genomic Insights into Virulence Factors and Multi-Drug Resistance in Clostridium perfringens IRMC2505A. Toxins (Basel). 2023;15. doi: 10.3390/toxins15060359. PubMed PMID: 37368661; PubMed Central PMCID: PMC10302382.
16 Welsh JA, Goberdhan DCI, O'Driscoll L, Buzas EI, Blenkiron C, Bussolati B, et al. Minimal information for studies of extracellular vesicles (MISEV2023): From basic to advanced approaches. J Extracell Vesicles. 2024;13:e12404. doi: 10.1002/jev2.12404. PubMed PMID: 38326288; PubMed Central PMCID: PMC10850029.
17 Clinical and Laboratory Standards Institute. CLSI document M07: Performance standards for antimicrobial susceptibility testing. 10th ed. Wayne (PA): CLSI; 2009.

18 Galvão I, de Carvalho RVH, Vago JP, Silva ALN, Carvalho TG, Antunes MM, et al. The role of annexin A1 in the modulation of the NLRP3 inflammasome. Immunology. 2020;160:78-89. doi: 10.1111/imm.13184. PubMed PMID: 32107769; PubMed Central PMCID: PMC7160667.
19 Krasnodembskaya A, Song Y, Fang X, Gupta N, Serikov V, Lee JW, et al. Antibacterial effect of human mesenchymal stem cells is mediated in part from secretion of the antimicrobial peptide LL-37. Stem Cells. 2010;28:2229-38. doi: 10.1002/stem.544. PubMed PMID: 20945332; PubMed Central PMCID: PMC3293245.
20 Lv H, Yuan X, Zhang J, Lu T, Yao J, Zheng J, et al. Heat shock preconditioning mesenchymal stem cells attenuate acute lung injury via reducing NLRP3 inflammasome activation in macrophages. Stem Cell Res Ther. 2021;12:290. doi: 10.1186/s13287-021-02328-3. PubMed PMID: 34001255; PubMed Central PMCID: PMC8127288.
21 Alam SI, Bansod S, Kumar RB, Sengupta N, Singh L. Differential proteomic analysis of Clostridium perfringens ATCC13124; identification of dominant, surface and structure associated proteins. BMC Microbiol. 2009;9:162. doi: 10.1186/1471-2180-9-162. PubMed PMID: 19664283; PubMed Central PMCID: PMC2731776.
22 Briolat V, Reysset G. Identification of the Clostridium perfringens genes involved in the adaptive response to oxidative stress. J Bacteriol. 2002;184:2333-43. doi: 10.1128/jb.184.9.2333-2343.2002. PubMed PMID: 11948145; PubMed Central PMCID: PMC134984.
23 Hooper DC, Jacoby GA. Topoisomerase Inhibitors: Fluoroquinolone Mechanisms of Action and Resistance. Cold Spring Harb Perspect Med. 2016;6. doi: 10.1101/cshperspect.a025320. PubMed PMID: 27449972; PubMed Central PMCID: PMC5008060.
24 Zhu JY, Yang Y, Han H, Betzi S, Olesen SH, Marsilio F, et al. Functional consequence of covalent reaction of phosphoenolpyruvate with UDP-N-acetylglucosamine 1-carboxyvinyltransferase (MurA). J Biol Chem. 2012;287:12657-67. doi: 10.1074/jbc.M112.342725. PubMed PMID: 22378791; PubMed Central PMCID: PMC3339971.
25 Shaaban F, Salem Sokhn E, Khalil C, Saleh FA. Antimicrobial activity of adipose-derived mesenchymal stromal cell secretome against methicillin-resistant Staphylococcus aureus. Stem Cell Res Ther. 2025;16:21. doi: 10.1186/s13287-025-04138-3. PubMed PMID: 39849590; PubMed Central PMCID: PMC11755800.
26 Li H, Ding Y, Huang J, Zhao Y, Chen W, Tang Q, et al. Angiopep-2 Modified Exosomes Load Rifampicin with Potential for Treating Central Nervous System Tuberculosis. Int J Nanomedicine. 2023;18:489-503. doi: 10.2147/ijn.s395246. PubMed PMID: 36733407; PubMed Central PMCID: PMC9888470.
27 Yang X, Shi G, Guo J, Wang C, He Y. Exosome-encapsulated antibiotic against intracellular infections of methicillin-resistant Staphylococcus aureus. Int J Nanomedicine. 2018;13:8095-104. doi: 10.2147/ijn.s179380. PubMed PMID: 30555228; PubMed Central PMCID: PMC6278838.